



## Effect of Radio Frequency Sputtering and Laser Remelting on Ti6Al4V Behavior in Medical Applications

M. A. Ali Bash<sup>a</sup>, A. N. Jasim<sup>b</sup>, A. M. Resin<sup>\*a</sup>, S. A. Ajeel<sup>a</sup>

<sup>a</sup> College of Production Engineering and Metallurgy, University of Technology, Baghdad 10066, Iraq

<sup>b</sup> Department of Materials Engineering, University of Diyala, Iraq

### PAPER INFO

#### Paper history:

Received 13 March 2025

Received in revised form 15 June 2025

Accepted 17 June 2025

#### Keywords:

Biomaterial

Corrosion

Radio Frequency Sputtering

Ti6Al4V

Laser Treatment

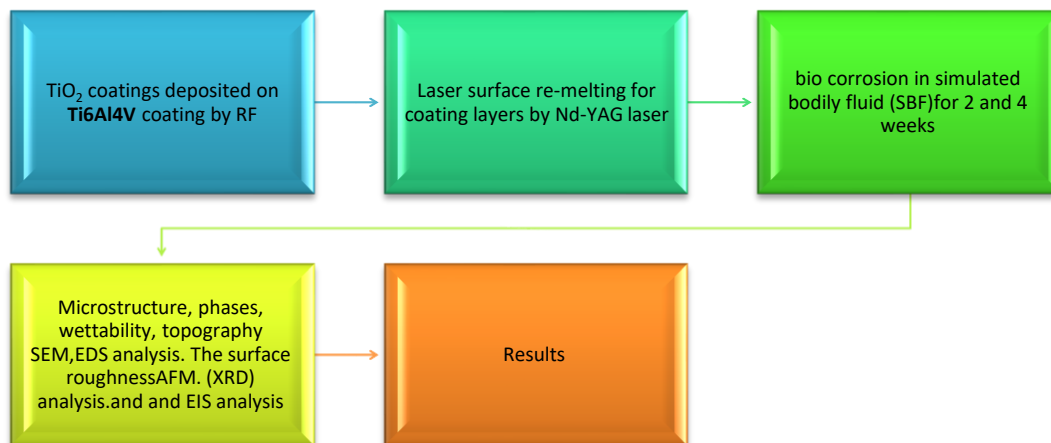
Electrochemical Impedance Spectroscopy

### ABSTRACT

In the field of orthopedics, the Ti6Al4V alloy is frequently used as a biomaterial, due to their characteristics such as high toughness, mechanical properties, high corrosion resistance, fracture toughness, biocompatibility and high strength. Yet, it has specific issues, such as corrosion and the release of vanadium element to the body fluids. Surface treatment methods promote osseointegration and biocompatibility by providing bioactivity and a barrier effect. In this study, the biological behavior of Sputtering titanium oxide (TiO<sub>2</sub>) using radio frequency magnetron sputtering (RF) method as well as laser remelting of the pre-sputtered Ti6Al4V surface was investigated using Nd: YAG laser. Microstructure, phases, wettability, topography, composition, bioactivity of the modified surfaces were characterized using SEM, XRD, EDS, roughness, hardness, electrochemical corrosion, and Electrochemical Impedance Spectroscopy (EIS) analysis. The results demonstrate that the behavior of the substrate was positively impacted by the application of both surfaces engineering techniques, including the sputtering of ceramic coating and surface modification by laser remelting treatment. The improvement is owing to the formation of bioactive and more resistant surfaces. The modification of the surface performs two functions. The first serves as a barrier that prevents body fluids from reaching the implant, and it also provides a surface roughness and porosity similar to the roughness of the bone surface for the growth of surrounding tissue.

doi: 10.5829/ije.2026.39.05b.08

### Graphical Abstract



\*Corresponding author email: [ali.m.resen@uotechnology.edu.iq](mailto:ali.m.resen@uotechnology.edu.iq) (A. M. Resin)

Please cite this article as: Ali Bash MA, Jasim AN, Resin AM, Ajeel SA. Effect of Acid Treatment and Clay Mineral Type on Acidic Clay Catalyst Performance in Esterification. International Journal of Engineering, Transactions B: Applications. 2026;39(05):1139-51.

## 1. INTRODUCTION

Titanium and its alloys gained widespread use in the biomedical industry, where biological characteristics such as low elastic modulus, good fatigue strength, formability, and corrosion resistance were of crucial significance (1-3). This material is preferred because of its exceptional strength-to-weight ratio and remarkable biocompatibility, which means the body accepts it well and does not react unfavorably (4-6). Due to its ability to tolerate the mechanical stresses encountered in daily activities, Ti6Al4V is frequently utilized in orthopedic devices, dental implants, and joint replacements (7-9). The long-term clinical research confirms Ti6Al4V good biocompatibility. However, it raised concerns that the cytotoxic component vanadium might be released and cause both local and systemic issues (10, 11). Long amounts of time spending in close contact with semi-planted cells might be dangerous (12). Biomedical applications must cover innovative materials to increase the functionality and longevity of medical devices. Recently, surface modification techniques have attracted attention because they may speed up or improve "bone-anchorage" by creating a bio-interface between the implant and the surrounding bone tissue (13-15). So, the implant's surface characteristics are critical for osteoblast adhesion and growth during the early stages of osseointegration as well as long-term bone remodeling (16, 17). In this instance, the methods that primarily utilized involve adjusting the implant's roughness and texture. Chemical and structural changes to the composition of the surface that make touch with the bone to facilitate a direct chemical connection, strengthening other physical elements like bone tissue guidance, biomechanical stability, and bone anchoring (18, 19).

Thereby, a variety of techniques have been employed to locally modify the implants' surface energy, biochemistry, and topography (20). Simultaneously, efforts have been taken to enhance the mechanical characteristics of implants, with particular emphasis on improving the hardness as well as improving the wear resistance of metallic implants (21). Radio frequency magnetron sputtering is a more attractive plasma/vacuum-based deposition technique in this regard. One of the most prevalent plasma technologies in industry for coating and surface modification is magnetron sputtering, which produces highly conformal coatings which adhere well to a wide range of substrates (22-24). Titanium oxide (TiO<sub>2</sub>) is a well-known coating material because of its exceptional biocompatibility, or

ability to live with living tissue without having an adverse impact (25, 26). For materials that come into direct contact with biological systems, this feature is essential. Another novel technique for modifying the surface features of Ti6Al4V is laser surface treatment (27-30). The surface can be melted and then resolidified with lasers, producing microstructures that improve the material's characteristics (31). This procedure may prolong the implant's lifespan overall, increases surface hardness, and reduce wear. Furthermore, by producing textured surfaces that simulate real bone, laser treatment can improve the osseointegration, which is the process by which bone cells attach to the implant surface (32). Improved osseointegration is vital for the success of implants. By tailoring the surface characteristics of Ti6Al4V, engineers and scientists can develop implants that not only perform better but also lead to enhance patient outcomes (33).

In this investigation, studying the impact of using combination of advanced surface treatment techniques like RF sputtering and laser treatment on Ti6Al4V surface were focused. Through a series of experiments and tests, the microstructural, phases, roughness, and biocorrosion resistance of the treated specimens were evaluated compared to the untreated standard.

## 2. EXPERIMENTAL

**2. 1. Coating of the Ti6Al4Vsubstrate** The experimental material used as substrate in this investigation is a plate of Ti6Al4V alloy 3 mm thick. Its chemical composition is demonstrated at Table 1. Ceramic coating is TiO<sub>2</sub> nano-coating using RF sputtering. Before RF sputtering, the surface of substrate materials was ground with 400-grit waterproof abrasive paper to increase the bonding between the substrate and ceramic coating. The sputtering chamber was evacuated to a working pressure of  $5 \times 10^{-3}$  mbar. The deposition of TiO<sub>2</sub> film was conducted using the RF sputtering system in a pure argon atmosphere (99.9%) at a pressure of  $5 \times 10^{-3}$  mbar for a duration of 90 minutes.

**2. 2. Laser Surface Re-melting of Ti6Al4V Pre-sputtered with TiO<sub>2</sub>** A Nd: YAG laser was applied to process the surface of Ti6Al4V pre -sputtered with TiO<sub>2</sub>. The processing parameters of the laser surface treatment were applied by frequency: 2 Hz, power: 650W, and traverse speed: 8 mm/s.

**TABLE 1.** The chemical composition of the standard Ti6Al4V alloy

Chemical element	Al	V	Fe	O	N	H	C	Ti
Standard (ASTM)	5.5/6.75	3.5/4.5	0.30	0.20	0.05	0.01	0.10	Balance

**2. 3. Wettability Measurements** The contact angle measurement method used to determine the wettability of the surface by the droplet suspension method with a contact angle tester type (Creating Nano Tech., Model: CAM110P, Serial No. 113031201804W). Less than a  $90^\circ$  angle of water contact corresponds to a hydrophilic surface, which is thought to promote the nutrients and cell attachments associated with bone formation.

**2. 4. Surface Roughness** Roughness can be described as the irregularity in surface profile that includes valleys and peaks, and it provides a significant impact on cellular responses (i.e., proliferation, differentiations, and adhesion) for implanting the surface. It has been evaluated using a Surface Roughness Tester type (JITAI8103Plus Surface Roughness Tester). The range was  $-80/80\mu\text{m}$  and the cutoff: 2.5mm. consists mostly of the contour's most significant height ( $R_z$ ), its arithmetic mean deviation ( $R_a$ ), and its root-mean-square deviation of the contour mean line ( $R_q$ ).

**2. 5. Analysis Methods** FESEM was utilized to characterize the surface of Ti6Al4V, after RF sputtering the surface with  $\text{TiO}_2$  and, after laser remelting of pre-sputtered Ti6Al4V. The compositions were analyzed with EDS analysis. As well as X-ray diffractometer (XRD) analysis used to identify the phases existing on the treated surfaces.

**2. 6. Biocorrosion Behavior and EIS Measurements** To investigate the behavior and corrosion rate of specimens in the simulated bodily fluid (SBF) for 2 and 4 weeks, electrochemical evaluations of the uncoated Ti6Al4V substrate,  $\text{TiO}_2$ -sputtered, and laser remelting of the pre-sputtered surface have been carried out. The corrosion rate was measured in millimeters per year (mm/y) using a CHI 604e electrochemical system. The AC impedance spectra for Ti6Al4V samples in simulated body fluids (SBF) were obtained. This analysis serves two purposes: first, it provides a diagnostic assessment of the surface's characteristics; second, it aids in the assessment of the enhancements that perform to overcome corrosive circumstances with frequencies up to 1 MHz.

### 3. RESULTS AND DISCUSSION

#### 3. 1. Microstructural Features of the Coatings

Figure 1 depicts typical FESEM micrograph images of Ti6Al4V after RF sputtering with  $\text{TiO}_2$  and laser surface remelting. The ceramic  $\text{TiO}_2$  films deposited on the surface of Ti6Al4V seemed thin since the grinding grooves of the substrate were still visible as shown in Figure 1(a, b). The grinding process of the substrate exhibited parallel grooves in the grinding direction to promotes the mechanical anchoring of coatings. Figure 1 (c, d) shows the laser surface remelting of pre-sputtered

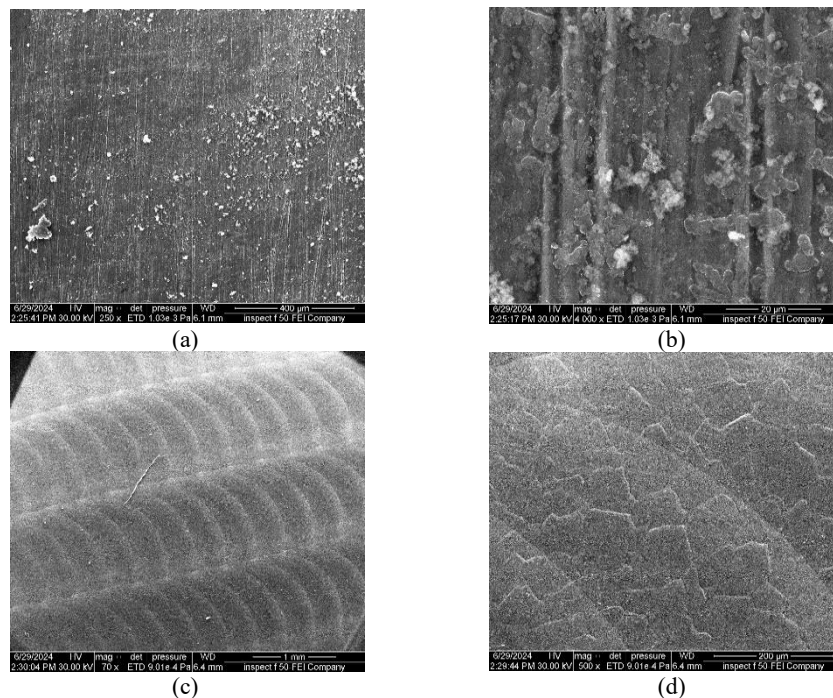


**Figure 1.** Plan view of Ti6Al4V after (a, and b) RF sputtering of  $\text{TiO}_2$  on the ground of Ti6Al4V surface at different magnifications (c, and d) laser remelting of the pre-sputtered Ti6Al4V surface

Ti6Al4V. It can observe the uniform laser tracks overlap according to the investigated parameters used in this paper. Also, the martensite phase of the Ti alloy can be clearly observed at high magnification of Figure 1(d). The martensite phase was performed due to the high cooling rate that occurred after laser treatment.

The interesting think is the presence of ceramic coating on the surface of metallic substrate. It is playing a two crucial role. The first one is in protecting the metallic surface of the implants. Because the ceramic nano coating considered more resistant to the surrounding environment from the mechanical and biological point. The second role in increasing the surface response of Ti6Al4V to the laser beam interaction. As it is known the response of metallic surface to the laser beam lesser than the ceramic one. In other words, the laser beam absorption in the case of ceramic coating is high. Therefore, control over surface details is better.

Figure 2 displays the XRD spectra of substrate Ti-6Al-4V and modified specimens. Ti6Al4V alloy before coating showed three different  $2\theta$  peaks are related for Ti6Al4V [32.76 $\theta$  (100), 35.24 $\theta$  (002) and 40.13  $\theta$  (101)]. They identified according to JCPDS card No 33-0397. Also, it is indicated that this structure includes ( $\alpha$ + $\beta$ ), while the  $\alpha$  phase is representing the  $\alpha$  stabilizing element as Al element has the tendency of stabilizing the  $\alpha$  phase, whereas (V) element is acting as  $\beta$  phase stabilizer.

There are no characteristic peaks of TiO<sub>2</sub> after RF sputtering of Ti-6Al-4V with TiO<sub>2</sub>. It disappears due to Titania which is a thin layer and it could not find by XRD analysis. But it can be characterized using GXR analysis of sputtering TiO<sub>2</sub> on the surface of glass as shown in Figure 3. It's important to note, after laser treatment, it can obtain martensitic phase ( $\alpha'$ ) as a result of high cooling rate. Such high cooling rates force formation of acicular martensite structure and enhances the materials wear and corrosion resistance (34). The

lattice plane spacing in the constituent grains changed from a stress-free value to a new value that matched the amount of stress applied when Ti6Al4V was subjected to laser treatment, which caused uniform strain to be generated over comparatively wide distances (Table 2).

The crystallinity of phases increases after laser treatment due to the high temperature of laser remelting of Ti6Al4V sputtered with TiO<sub>2</sub>. There are no characteristic peaks of TiO<sub>2</sub> after laser remelting of pre-sputtering of Ti-6Al-4V with TiO<sub>2</sub>. Table 2 lists the crystalline size for Ti6Al4V before and after modification.

**3. 2. Surface Wettability of Titanium Alloy** The biological system is significantly affected by the wettability of implant surfaces, including protein adhesion, surface interactions with hard and soft tissue cells, bacterial affinity, and biofilm formation. Figure 4 depicts the surface samples' wetting behavior. As previously noted, the contact angle of water droplets on the specimen surface was used to assess the wettability of the Ti6Al4V alloy under all conditions. Prior to coating, the ground substrate Ti6Al4V alloy had a contact angle value of 70.415. The value of the contact angle increased to 101.637 upon the application of TiO<sub>2</sub> coating via RF sputtering on the Ti6Al4V surface. This indicates that, in comparison to the surface without coating, the Ti alloy surface became hydrophobic.

However, the pre-sputtered Ti6Al4V surface's contact angle value dropped to 79.538 during laser remelting. Figure 4 shows that after laser remelting, the surface wettability of the titanium alloy increased and the CA value dropped. This may be explained by the fact that the water droplets are stored in the groove structure at a specific depth as a result of laser track overlapping, which facilitates their spreading across the titanium alloy surface and results in a reduced contact angle (33).

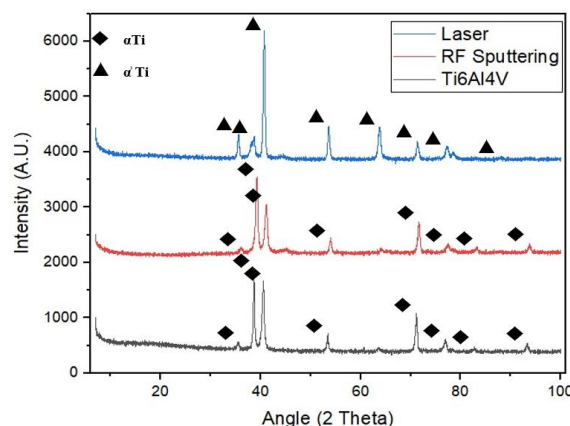


**Figure 2.** The XRD analysis of the substrate (Ti6Al4V), RF sputtering of TiO<sub>2</sub>, and laser remelting of pre-sputtered substrate

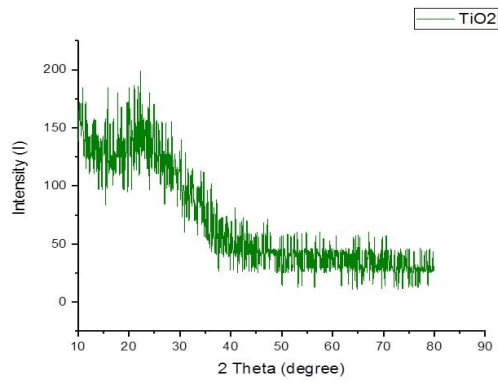


**Figure 3.** GXRDR curve of sputtering TiO<sub>2</sub> on the surface of glass

Surface wettability plays a crucial role during the insertion of an implant into the body. Additionally, the process governs the adsorption of the proteins, which is followed by cell attachments. It appears that on hydrophilic surfaces as opposed to hydrophobic ones, the cells will be attached and grow (33).

Surface roughness was obtained for the specimens of Ti6Al4V alloy and after RF sputtering with TiO<sub>2</sub> and laser surface remelting as shown in Table 3 and Figure 5. It shows the surface roughness profiles of the specimens. It can observe that the condition with ceramic nano coating using the magnetron RF sputtering reduces surface roughness of the Ti6Al4V alloy to (0.344 μm) and improved integrity compared to the substrate

**TABLE 2.** The FWHM and crystalline size of the three specimens

ITEM	FWHM	Area	Crystallite size(A°)	Micro Strain [%]
substrate (Ti6Al4V)	0.2642	413.09	296	0.39288
After RF sputtering of Ti6Al4V	0.4607	661.22	152	0.75423
After Laser surface treatment of pre- sputtered Ti6Al4V	0.6648	135.64	101	1.16361

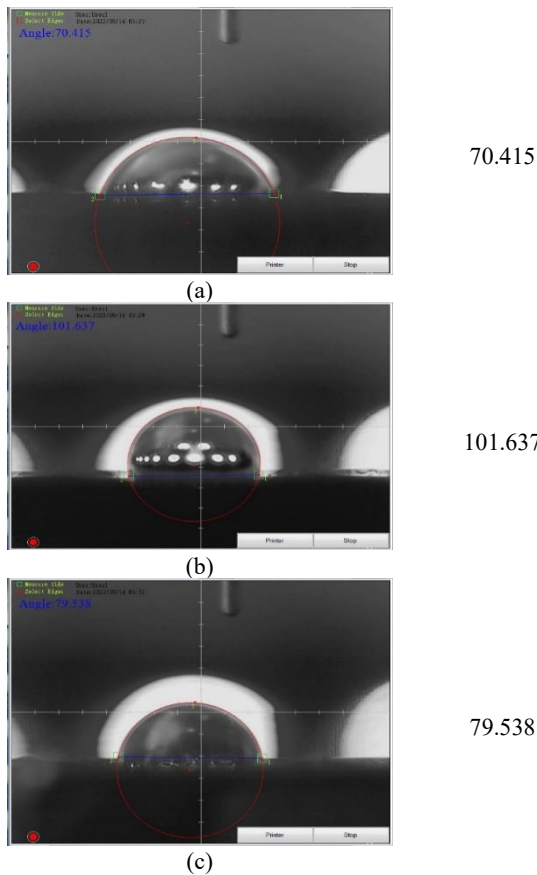


**Figure 4.** The water contact angle measurements of (a) Ground substrate (Ti6Al4V) (b) After RF sputtering of Ti6Al4V (c) After Laser surface treatment of pre- sputtered Ti6Al4V

condition after grinding with abrasive paper (1.522 μm). This attributed to the filling the grooves that generated due to the grinding paper with the ceramic coating materials (TiO<sub>2</sub>) and that agree with reported data (35). On the other hand, the surface roughness increases after laser surface remelting of pre-sputtered Ti6Al4V to (4.581 μm). Because, the surface texture that generated after overlapping of laser track results in the increasing of roughness values. As well as, the laser processing parameters used in this investigation by Naji et al. (33). It is important to note that increasing the surface roughness to some extent was preferred for some of the biological tests, such as bioactivity, that improve osseointegration.

**3. 3. Microstructure after Bioactivity**

The surface bioactivity is an aspect of high importance for ensuring subsequent bone implant integration in terms of in vivo conditions, thus three distinctive samples (Ti6Al4V alloy surface, RF sputtering of TiO<sub>2</sub> on the surface of Ti6Al4V, and laser surface remelting of pre-sputtered Ti6Al4V with TiO<sub>2</sub>) were specified via immersion in the SBF for 2 and 4 weeks. The (FE-SEM)

**TABLE 3.** Surface roughness for Ti6Al4V samples

Samples	R <sub>a</sub> (μm)	R <sub>z</sub> (μm)	R <sub>q</sub> (μm)
Ground substrate (Ti6Al4V)	1.522	9.96	1.978
After RF sputtering of Ti6Al4V	0.344	2.796	0.448
After Laser surface treatment of pre- sputtered Ti6Al4V	4.581	17.596	5.258

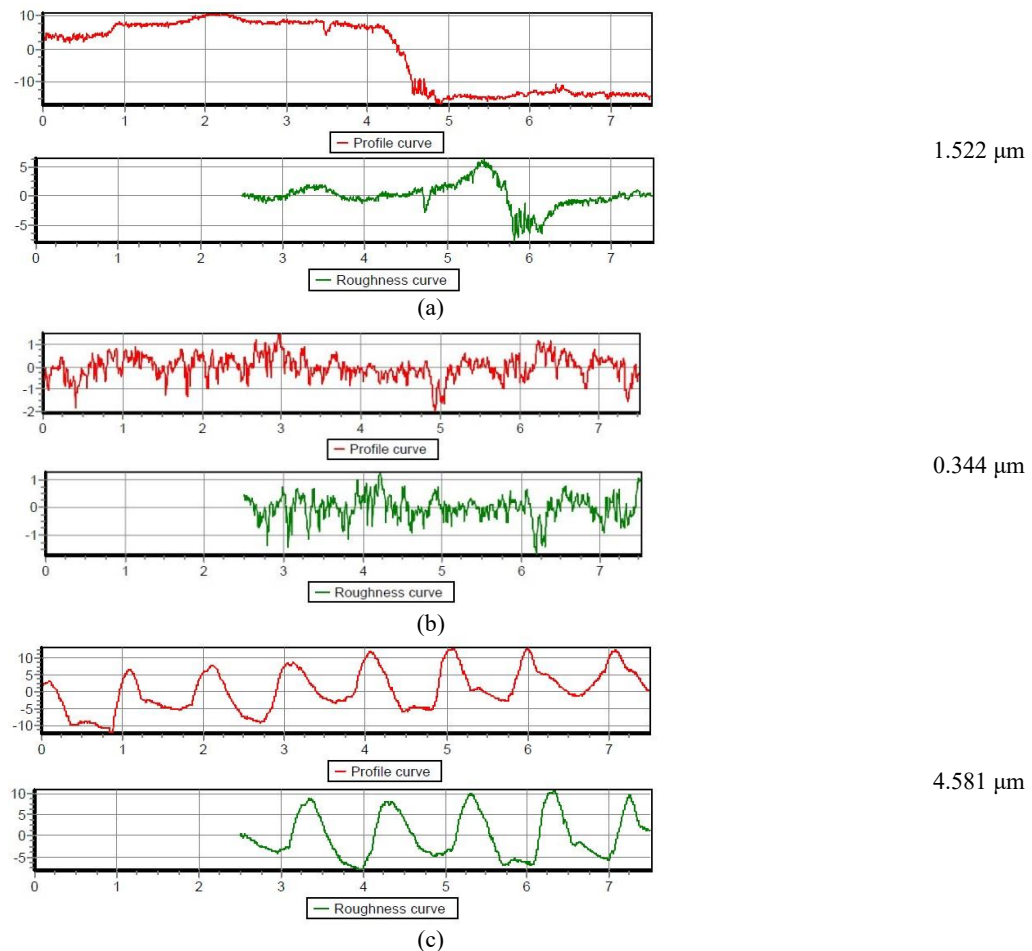


**Figure 5.** Surface roughness profilometer of titanium alloy samples at the condition: (a) Ground substrate (Ti6Al4V) (b) After RF sputtering of Ti6Al4V (c) After Laser surface treatment of pre-sputtered Ti6Al4V

analysis visually assesses the morphological features of all cases investigated in this study. The FE-SEM micrograph clearly shows the apatite formation on the surfaces of the samples. Figure 6(a) indicates the surface of titanium alloy Ti6Al4V covered with a thin layer of hydroxyapatite with random distribution. while Figure 6(b) shows that almost the TiO<sub>2</sub> nano-coating surface had been covered with apatite in semi-equal distribution. The surface will be denser and thicker because of an increase in the nucleation of the apatite, indicates a creating a layer of the apatite on the surface related to mineralized bio ceramic material types.

Also, on the surface of the laser-treated of pre-sputtered samples in Figure 6(c), there is a homogeneity in apatite formation and some aggregation highlight the success of the synthesis process in achieving a uniform distribution. These results suggest that bone formation depends on the type of materials and surface nature. It is significant that after laser surface remelting, the apatite formation was better than that of both Ti6Al4V surface

and sputtered surface with TiO<sub>2</sub>. The existence of overlapping regions after laser surface treatment promotes the growth, density, and cell survival rate. Moreover, Figure 7 at high magnification shows that all region on the surface was covered with bone structure. Which means the surfaces after laser treatment have high activation energy and nucleation sites for bone formation.

This indicates that osteointegration may response differently to different surface structure. In addition, the surface energy and surface roughness would be essential factors for facilitating the cells adhesion and proliferation. It's important to note this study deals with laser-treated surfaces after ceramic coating which means responding and absorbing the laser beam with high efficiency.

Figure 8 shows the microscopic morphology and the corresponding chemical composition obtained from EDS analysis on the titanium alloy after laser treatment. The SEM-elemental mapping in Figure 8 illustrates the existence of bone elements Ca, P, and O. Highlighting

the successful osteointegration process on the surface of the sample. Also, the XRD pattern confirms the formation of apatite on the surface of all specimens in

Figure 9. The HA peaks were identified according to JCPDS card No 96-230-0274.

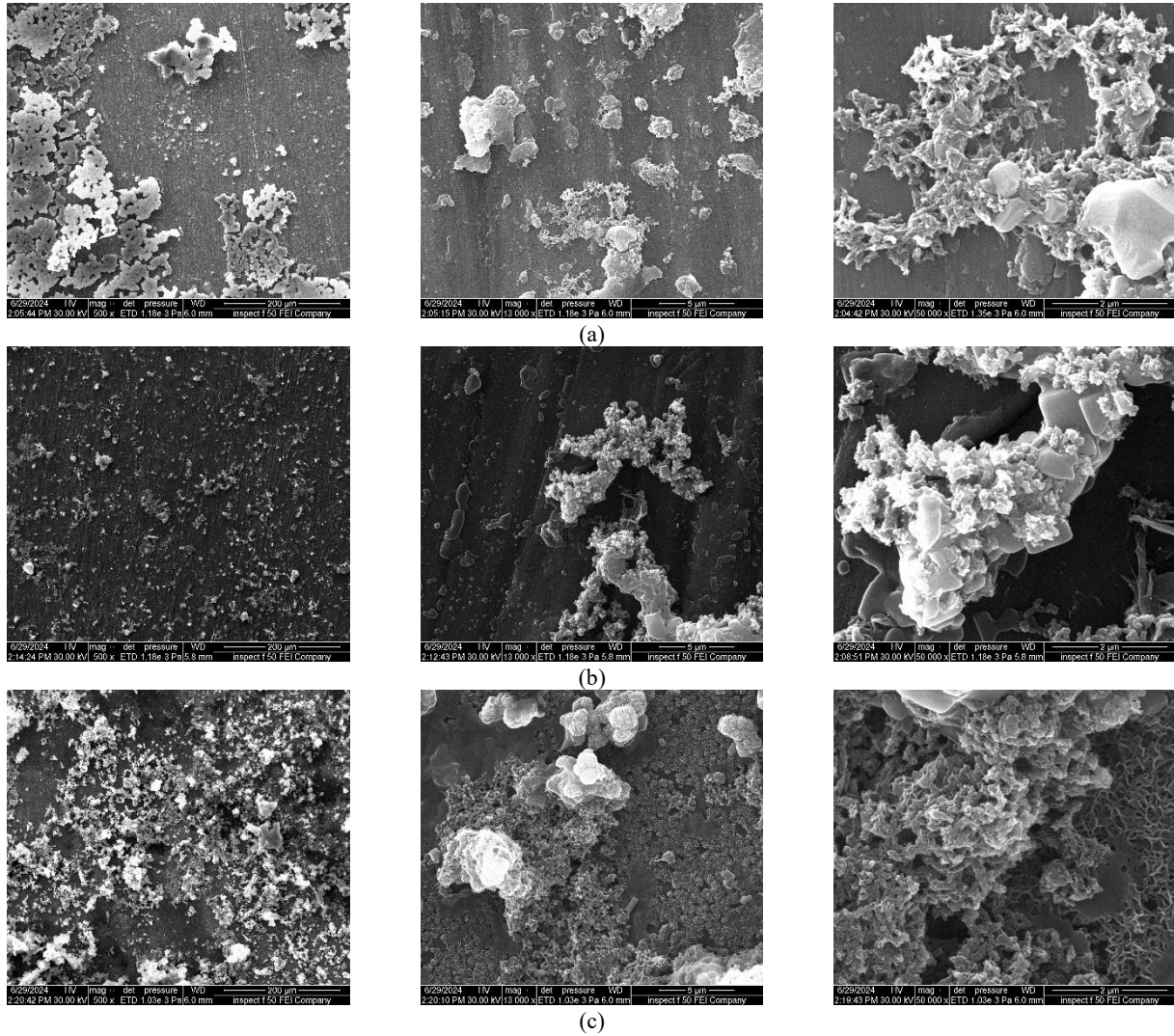


**Figure 6.** FE-SEM images of bone formation on three different samples for 7 days (a) Ti6Al4V substrate (b) RF sputtered surface of Ti6Al4V with TiO<sub>2</sub> (c) Laser surface remelting of pre-sputtered Ti6Al4V with TiO<sub>2</sub>

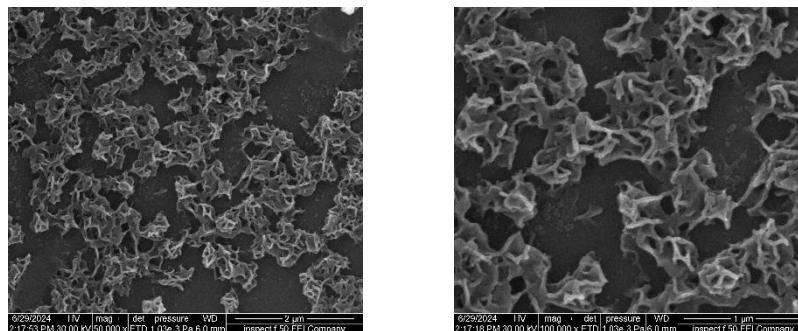


**Figure 7.** High magnification of laser treated surface showing the bone formation

3. 4. EDS Analysis

3. 5. Tafel Results Discussion

To evaluate the effect of TiO<sub>2</sub> sputtering and laser treatment of pre-sputtered surface on the corrosion resistance of the titanium alloy (Ti6Al4V), the electrochemical corrosion performance of the samples in the SBF solution was tested. Also, the electrochemical corrosion performance was conducted for all samples after immersion in SBF for 4 weeks to simulate the investigated samples in human body as implants. The results are shown in Figure 10. The open circuit potential (OCP), corrosion current density (I<sub>corr</sub>), corrosion potential (E<sub>corr</sub>), and inhibition efficiency were calculated and summarized in Table 4. The values of OCP were nobler with (-0.128 and -0.241) volt when sputtered the Ti6Al4V with TiO<sub>2</sub> and surface laser remelting of pre-sputtered surface if compared with the OCP value for untreated Ti6Al4V (-0.515) volt.

The Tafel curve in Figure 10(a) demonstrates the improvement in corrosion behavior after using both two methods of surface engineering for Ti6Al4V. A reduced current density and a larger corrosion potential confirmed this in Table 4. So, the values of corrosion rate decreased from (3.255 × 10<sup>-2</sup>) to (3.892 × 10<sup>-3</sup>) and (1.079 × 10<sup>-2</sup>) mm/y. Due to the protection that comes from the surface treatment, which creates a noble transition compared to the untreated substrate. Moreover, these methods exhibited a higher inhibition efficiency 88.04% and 66.85% respectively. This enhancement is attributed to the application of a ceramic layer from titania which considered excellent corrosion resistance. It's important to note the improvement after sputtering is higher than the improvement following laser remelting treatment of pre-sputtered surface. The reason for this is that overlapping occurs during laser treatment, as shown in

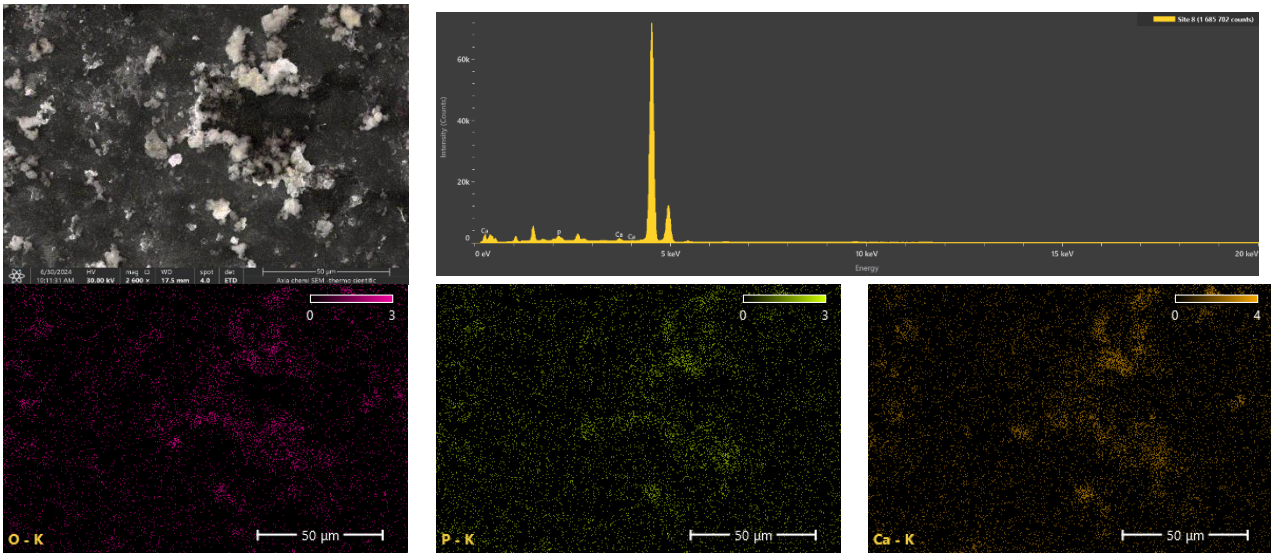


Figure 8. EDS analysis and SEM-elemental mapping after immersion in SBF solution of the laser remelted pre-sputtered Ti6Al4V exhibit the existence of HA on the surface

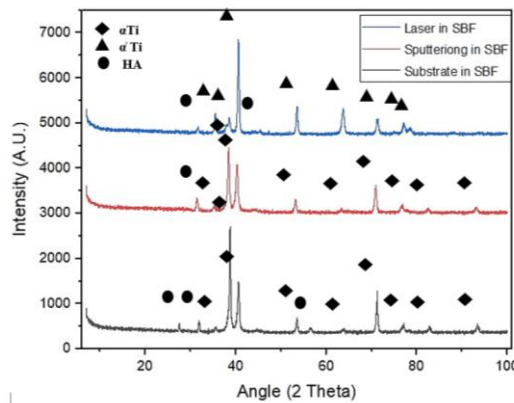
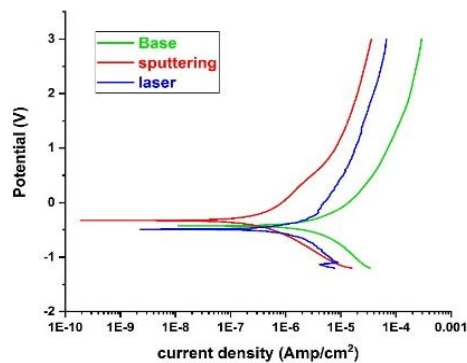


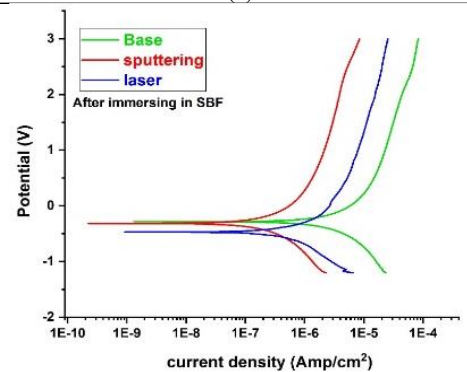
Figure 9. XRD analysis of the three cases after immersion in SBF solution for 2 weeks

TABLE 4. Electrochemical corrosion results

ITEM	E corr. (volt)	I corr. (Amp.)	Corr. Rate (mmpy)	$\beta_c$	$\beta_a$	OCP (volt)	$\eta\%$
Base	-0.429	$1.440 \times 10^{-6}$	$3.255 \times 10^{-2}$	0.206	0.204	-0.515	---
Base in SBF	-0.278	$8.659 \times 10^{-7}$	$1.957 \times 10^{-2}$	0.212	0.204	0.290	39.87%
Sputtering	-0.319	$1.722 \times 10^{-7}$	$3.892 \times 10^{-3}$	0.188	0.206	-0.128	88.04%
Sputtering in SBF	-0.323	$6.540 \times 10^{-8}$	$1.478 \times 10^{-3}$	0.206	0.185	0.119	95.45%
Laser after sputtering	-0.493	$4.774 \times 10^{-7}$	$1.079 \times 10^{-2}$	0.212	0.210	-0.241	66.85%
Laser after sputtering in SBF	-0.490	$2.131 \times 10^{-7}$	$4.817 \times 10^{-3}$	0.206	0.184	0.162	85.20%



(a)



(b)

**Figure 10.** Anticorrosion measurements on the Ti6Al4V alloy of the three different samples (a) before and (b) after immersion in SBF solution for 4 weeks

Figure 1, resulting in an increase in surface roughness in the overlapping area and subsequently an increase in the surface area exposed to corrosion solution. Furthermore, the generation of residual stresses as well as the small grain sizes results due to rapid solidification rate after laser treatment suggested the cause of a reduction in corrosion resistance slightly compared to the case of sputtering.

While the OCP, Tafel curve results for the three investigated specimens after immersion in SBF solution for 4 weeks demonstrate more enhancement in corrosion behavior as shown in Figure 10(b). The OCP values was 0.119 and 0.162 compared to the value of the substrate

0.290. The corrosion rate also decreased after immersion in SBF solution to ( $1.478 \times 10^{-3}$ ) and ( $4.817 \times 10^{-3}$ ), respectively compared to the substrate corrosion rate after immersion in SBF ( $1.957 \times 10^{-2}$ ) mm/y., which attributed to the formation of HA film of the surface of the samples play as a barrier against direct contact to the solution. Which means the reduction of corrosion of implants due to the osseointegration of bones. The inhabitation efficiency also increases to 95.45% and 85.20% as well as for the substrate become 39.87% after immersion in SBF solution compared to the values before immersion. These results reflect the performance of implants with the progress of time.

### 3. 6. EIS Analysis

EIS is a method that is especially sensitive to minor system changes and facilitates for the characterization of material properties and electrochemical process mechanisms. The Nyquist graphs (see Figure 11 and Table 5) demonstrate the electrochemical corrosion performance of the samples in the SBF solution to find out the impact of TiO<sub>2</sub> sputtering and laser treatment of the pre-sputtered surface on the titanium alloy's (Ti6Al4V) corrosion resistance (Figure 11 (a, c, e)). In order to replicate the examined materials in the human body as implants, an electrochemical corrosion performance assessment was additionally carried out on all samples following a 4-week immersion in SBF (Figure 11(b, d, f)).

It is obvious from the diagrams that the base metal's (Ti6Al4V) impedance response was 9858  $\Omega$  (Figure 11(a)). The solution resistant is denoted by  $R_1 = 207 \Omega$ , and the double layer resistant by  $R_2 = 9651 \Omega$ . While after sputtering of nano ceramic layer type titania oxide, the value of the impedance became 255733  $\Omega$  (Figure 11(c)). The solution resistant is denoted by  $R_1 = 217 \Omega$ , the TiO<sub>2</sub> ceramic layer resistant is denoted by  $R_2 = 242943 \Omega$ . High adhesion, a strong atomic bond, and a low pore rate are characteristics of this layer.  $R_3 = 12573 \Omega$  for the double layer resistant. As long as  $R_2$  is linked to  $R_3$ , this means that there are pores in the layer, but within an acceptable limit. After laser remelting of pre-sputtered with TiO<sub>2</sub> of the base metal, the value of impedance response was 56741  $\Omega$  (Figure 11(e)). The solution resistant is denoted by  $R_1 = 200 \Omega$ , and there were two separated

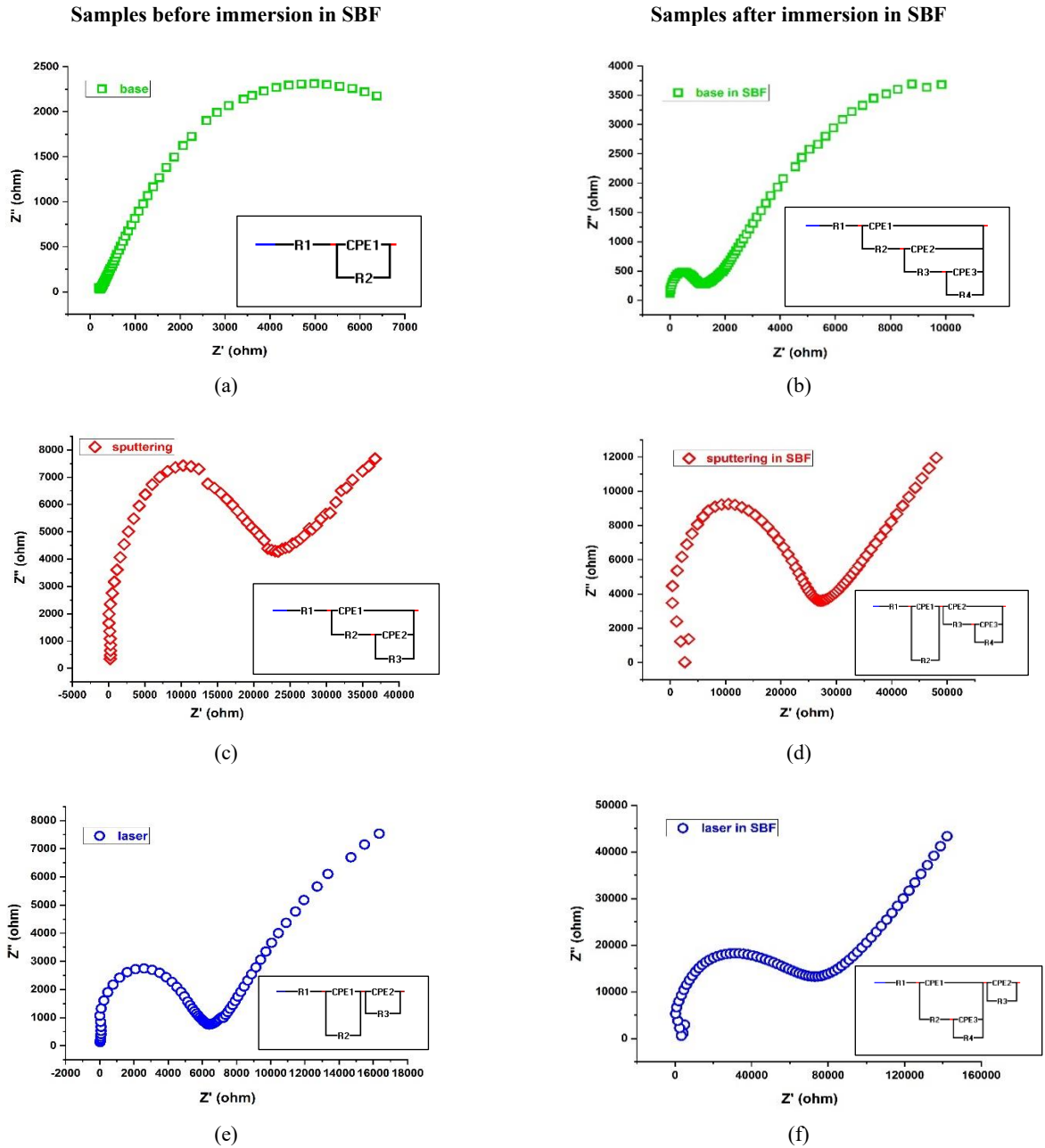


**Figure 11.** Nyquist plot of Ti6Al4V implant alloy in SBF solution (a) Base metal (Ti6Al4V) (b) Base metal in SBF (c) After sputtering of TiO<sub>2</sub> (d) After sputtering of TiO<sub>2</sub> in SBF (e) Laser after sputtering (f) Laser after sputtering in SBF

**TABLE 5.** EIS analysis for the investigated samples

Samples type	Total Impedance(ohm)	R1 (ohm)	R2(ohm)	R3(ohm)	R4(ohm)
Base	9858	207	9651	----	----
Base in SBF	40062	232	34816	3576	1438
Sputtering	255733	217	242943	12573	----
Sputtering in SBF	1.172472e+6	228	1E06	1.639E-05	8334
Laser after sputtering	56741	200	50611	5930	----
Laser after sputtering in SBF	158263	214	1.0012E05	4.9012E04	8917

layers formed  $R_2=50611\Omega$  and  $R_3= 5930\Omega$  (the double layer resistant). The  $R_2$  corresponds to the effect of laser beam on the pre-sputtered surface.

The impedance spectra for Ti6Al4V implant alloys after immersion for 4 weeks in SBF solution (after apatite formation) are comprised of three semicircle loops (Figure 11 (b)). The solution resistant is denoted by  $R_1 = 232\Omega$ , the HA layer resistant by  $R_2 = 34816\Omega$ , the titanium oxide film formed as a result of sintering the HA layer in the furnace at  $400^\circ\text{C}$  after immersion in SBF solution by  $R_3= 3576\Omega$ , and the double layer resistant by  $R_4 = 1438\Omega$ . These findings show that the apatite layer (HA), which is thought to act as a barrier that improves the metal's resistance to corrosion, emerges as time passes, causing the rate of corrosion in the (SBF) solution to decrease. When compared to the resistance value prior to immersion, the titanium alloy's resistance rose to ( $40062\Omega$ ) after immersion. The EIS results for the titanium alloy's sputtered surface with titanium revealed varying levels of corrosion resistance (see Figure 11 (d)). The overall impedance increases to  $1.172472e+6\Omega$ , indicating that the surface of Ti6Al4V is difficult for the SBF solution to attack. The apatite layer that developed on top of the titanium layer ( $R_2=1E06$ ), which has a high density and is strongly bound to the surface, was primarily responsible for the high resistance. The impedance value after laser treatment of the surface sputtered with titanium after 4 weeks of immersion in the solution was  $158263\Omega$  Figure 11(f). Likewise, the resistance resulting from the apatite layer ( $R_2=1.0012E05\Omega$ ) is greater than the resistance to the laser effect on the material ( $R_3= 4.9012E04\Omega$ ). We conclude that in all the mentioned cases, the resistance values increase over time as a result of the compatibility and osseointegration provided by the mentioned materials.

#### 4. CONCLUSIONS

1. A uniform remelting surface can be achieved using Nd- YAG laser after sputtering of the ceramic layer from  $\text{TiO}_2$  on the surface of the base metal (Ti6Al4V). The laser – Ti6Al4V interaction increased after sputtering of ceramic layer.
2. XRD results reveal the formation of martensite phase  $\alpha'$  after laser treatment due to the rapid solidification instead of  $\alpha$  phase.
3. Biocompatibility increases after both sputtering and laser treatment of the Ti6Al4V surface.
4. For certain biological tests, as bioactivity, which seemed to indicate a method of improved osseointegration, it was preferable to increase the surface roughness to a certain degree. For laser surface remelting of pre-sputtered Ti6Al4V, the roughness was  $4.581\mu\text{m}$ .

5. EIS technique reflects the electrochemical corrosion of the investigated specimens. RF sputtering of  $\text{TiO}_2$  and laser surface remelting increase the values of impedance to the high level. The highest one was after sputtering of ceramic layer on the surface of Ti6Al4V.

#### 5. REFERENCES

1. Wiatrowski A, Mazur M, Obstarczyk A, Kaczmarek D, Pastuszek R, Wojcieszak D, et al. Influence of magnetron powering mode on various properties of  $\text{TiO}_2$  thin films. *Mater Sci Pol*. 2018;36:748-60. 10.2478/msp-2018-0099
2. Sobieszczek S. Surface modifications of Ti and its alloys. *Advances in Materials Science*. 2010;10:29-42. 10.2478/v10077-010-0003-3
3. Souza JC, Apaza-Bedoya K, Benfatti CA, Silva FS, Henriques B. A comprehensive review on the corrosion pathways of titanium dental implants and their biological adverse effects. *Metals*. 2020;10(9):1272. 10.3390/met10091272
4. Xue T, Attarilar S, Liu S, Liu J, Song X, Li L, et al. Surface modification techniques of titanium and its alloys to functionally optimize their biomedical properties: thematic review. *Frontiers in bioengineering and biotechnology*. 2020;8:603072. 10.3389/fbioe.2020.603072
5. Avcu E, Avcu YY, Baştan FE, Rehman MAU, Üstel F, Boccaccini AR. Tailoring the surface characteristics of electrophoretically deposited chitosan-based bioactive glass composite coatings on titanium implants via grit blasting. *Progress in organic coatings*. 2018;123:362-73. 10.1016/j.porgcoat.2018.07.021
6. Hanawa T. Biocompatibility of titanium from the viewpoint of its surface. *Science and Technology of Advanced Materials*. 2022;23(1):457-72. 10.1080/14686996.2022.2106156
7. Abd-Elaziem W, Darwish MA, Hamada A, Daoush WM. Titanium-Based alloys and composites for orthopedic implants Applications: A comprehensive review. *Materials & Design*. 2024;241:112850. 10.1016/j.matdes.2024.112850
8. Quinn J, McFadden R, Chan C-W, Carson L. Titanium for orthopedic applications: an overview of surface modification to improve biocompatibility and prevent bacterial biofilm formation. *IScience*. 2020;23(11). 10.1016/j.isci.2020.101745
9. Xu Y, Gao J, Huang Y, Rainforth WM. A low-cost metastable beta Ti alloy with high elastic admissible strain and enhanced ductility for orthopaedic application. *Journal of Alloys and Compounds*. 2020;835:155391. 10.1016/j.jallcom.2020.155391
10. Bandyopadhyay A, Mitra I, Goodman SB, Kumar M, Bose S. Improving biocompatibility for next generation of metallic implants. *Progress in materials science*. 2023;133:101053. 10.1016/j.pmatsci.2022.101053
11. Willis J, Li S, Crean SJ, Barrak FN. Is titanium alloy Ti-6Al-4 V cytotoxic to gingival fibroblasts—A systematic review. *Clinical and experimental dental research*. 2021;7(6):1037-44. 10.1002/cre2.444
12. Ektessabi A, Otsuka T, Tsuboi Y, Yokoyama K, Albrektsson T, Sennerby L, et al. Application of micro beam PIXE to detection of titanium ion release from dental and orthopaedic implants. *International Journal of PIXE*. 1994;4(02n03):81-91. 10.1142/S0129083594000118
13. Tuikampee S, Chaijareenont P, Rungsiyakull P, Yavirach A. Titanium surface modification techniques to enhance osteoblasts

- and bone formation for dental implants: a narrative review on current advances. *Metals*. 2024;14(5):515. 2075-4701/14/5/515
14. Kligman S, Ren Z, Chung C-H, Perillo MA, Chang Y-C, Koo H, et al. The impact of dental implant surface modifications on osseointegration and biofilm formation. *Journal of clinical medicine*. 2021;10(8):1641. 10.3390/jcm10081641
  15. Li J, Zhou P, Attarilar S, Shi H. Innovative surface modification procedures to achieve micro/nano-graded Ti-based biomedical alloys and implants. *Coatings*. 2021;11(6):647. 10.3390/coatings11060647
  16. Al-Zubaidi SM, Madfa AA, Mufadhil AA, Aldawla MA, Hameed OS, Yue X-G. Improvements in clinical durability from functional biomimetic metallic dental implants. *Frontiers in Materials*. 2020;7:106. 10.3389/fmats.2020.00106
  17. Zhang LC, Chen LY. A review on biomedical titanium alloys: recent progress and prospect. *Advanced engineering materials*. 2019;21(4):1801215. 10.1002/adem.201801215
  18. Sánchez-López JC, Rodríguez-Albelo M, Sánchez-Pérez M, Godinho V, López-Santos C, Torres Y. Ti6Al4V coatings on titanium samples by sputtering techniques: Microstructural and mechanical characterization. *Journal of Alloys and Compounds*. 2023;952:170018. 10.1016/j.jallcom.2023.170018
  19. Liu X, Chu PK, Ding C. Surface modification of titanium, titanium alloys, and related materials for biomedical applications. *Materials Science and Engineering: R: Reports*. 2004;47(3-4):49-121. 10.1016/j.mser.2004.11.001
  20. García-Cabezón C, Godinho V, Salvo-Comino C, Torres Y, Martín-Pedrosa F. Improved corrosion behavior and biocompatibility of porous titanium samples coated with bioactive chitosan-based nanocomposites. *Materials*. 2021;14(21):6322. 10.3390/ma14216322
  21. Frutos E, Karlik M, Polcar T. The role of  $\alpha$  "orthorhombic phase content on the tenacity and fracture toughness behavior of Ti-22Nb-10Zr coating used in the design of long-term medical implants. *Applied Surface Science*. 2019;464:328-36. 10.1016/j.apsusc.2018.09.017
  22. Prosolov KA, Lastovka VV, Khimich MA, Chebodaeva VV, Khlusov IA, Sharkeev YP. RF magnetron sputtering of substituted hydroxyapatite for deposition of biocoatings. *Materials*. 2022;15(19):6828. 10.3390/ma15196828
  23. Garg R, Gonuguntla S, Sk S, Iqbal MS, Dada AO, Pal U, et al. Sputtering thin films: Materials, applications, challenges and future directions. *Advances in colloid and interface science*. 2024;330:103203. 10.1016/j.cis.2024.103203
  24. Jafari S, Mahyad B, Hashemzadeh H, Janfaza S, Gholikhani T, Tayebi L. Biomedical applications of TiO<sub>2</sub> nanostructures: recent advances. *International journal of nanomedicine*. 2020:3447-70. 10.2147/IJN.S249441
  25. Kumaravel V, Nair KM, Mathew S, Bartlett J, Kennedy JE, Manning HG, et al. Antimicrobial TiO<sub>2</sub> nanocomposite coatings for surfaces, dental and orthopaedic implants. *Chemical Engineering Journal*. 2021;416:129071. 10.1016/j.cej.2021.129071
  26. Geng Y, McCarthy É, Brabazon D, Harrison N. Ti6Al4V functionally graded material via high power and high speed laser surface modification. *Surface and Coatings Technology*. 2020;398:126085. 10.1016/j.surfcoat.2020.126085
  27. Kolarovszki B, Ficsor S, Frank D, Katona K, Soos B, Turzo K. Unlocking the potential: laser surface modifications for titanium dental implants. *Lasers in Medical Science*. 2024;39(1):162. 10.1007/s10103-024-04076-1
  28. Sypniewska J, Szkodo M. Influence of laser modification on the surface character of biomaterials: titanium and its alloys—a review. *Coatings*. 2022;12(10):1371. 10.3390/coatings12101371
  29. Jażdżewska M, Majkowska-Marzec B, Ostrowski R, Olive J-M. Influence of surface laser treatment on mechanical properties and residual stresses of titanium and its alloys. *Advances in Science and Technology Research Journal*. 2023;17(6). 10.12913/22998624/172981
  30. Bash A, Resen AM, Atiyah A, Jasim K. Effect of Yb-YAG Laser Parameters on the Operating Regime of Plasma Sprayed NiCrAlY Premixed Coatings. *Progress in Color, Colorants and Coatings*. 2024;17(2):145-58. 10.30509/pccc.2023.167180.1240
  31. Wang C, Tian P, Cao H, Sun B, Yan J, Xue Y, et al. Enhanced biotribological and anticorrosion properties and bioactivity of Ti6Al4V alloys with laser texturing. *ACS omega*. 2022;7(35):31081-97. 10.1021/acsomega.2c03166
  32. Sun X, Lin H, Zhang C, Huang R, Liu Y, Zhang G, et al. Improved osseointegration of selective laser melting titanium implants with unique dual micro/nano-scale surface topography. *Materials*. 2022;15(21):7811. 10.3390/ma15217811
  33. Naji T ABM, Resen A. . Laser Scanning Speed Influences on Assessment of Laser Remelted Commercially Pure Titanium Grade 2. *International Journal of Engineering Transactions A: Basics*. 2024 37(1):178-86. 10.5829/ije.2024.37.01a.16
  34. Melero HC, Sakai RT, Vignatti CA, Benedetti AV, Fernández J, Guilemany JM, et al. Corrosion resistance evaluation of HVOF produced hydroxyapatite and TiO<sub>2</sub>-hydroxyapatite coatings in Hanks' solution. *Materials Research*. 2018;21(2):e20170210. 10.1590/1980-5373-mr-2017-0210
  35. Alibash M, Resen AM, Kareem A, Muhi Abdulsahib Y. Improving the Hot Corrosion Behavior of Plasma-sprayed MCrAlY by RF Sputtering of TiO<sub>2</sub> Nano-Coating and Laser Remelting Treatment. *Progress in Color, Colorants and Coatings*. 2024;17(1):27-38. 10.30509/pccc.2023.167142.1221

**COPYRIGHTS**

©2026 The author(s). This is an open access article distributed under the terms of the Creative Commons Attribution (CC BY 4.0), which permits unrestricted use, distribution, and reproduction in any medium, as long as the original authors and source are cited. No permission is required from the authors or the publishers.

**Persian Abstract****چکیده**

در زمینه ارتوپدی، آلیاژ  $Ti6Al4V$  به دلیل ویژگی‌هایی مانند چقرمگی بالا، خواص مکانیکی، مقاومت در برابر خوردگی بالا، چقرمگی شکست، زیست سازگاری و استحکام بالا، اغلب به عنوان یک زیست ماده مورد استفاده قرار می‌گیرد. با این حال، این آلیاژ دارای مشکلات خاصی مانند خوردگی و آزاد شدن عنصر وانادیوم به مایعات بدن است. روش‌های عملیات سطحی با فراهم کردن زیست فعالی و اثر سدگری، باعث بهبود اتصال استخوانی و زیست سازگاری می‌شوند. در این مطالعه، رفتار بیولوژیکی اکسید تیتانیوم اسپاترینگ ( $TiO_2$ ) با استفاده از روش اسپاترینگ مگنترون فرکانس رادیویی (RF) و همچنین ذوب مجدد لیزری سطح  $Ti6Al4V$  از پیش اسپاترینگ شده با استفاده از لیزر Nd: YAG بررسی شد. ریزساختار، فازها، ترشوندگی، توپوگرافی، ترکیب، زیست فعالی سطوح اصلاح شده با استفاده از SEM, XRD, EDS, زبری، سختی، خوردگی الکتروشیمیایی و آنالیز طیف‌سنجی امپدانس الکتروشیمیایی (EIS) مشخص شد. نتایج نشان می‌دهد که رفتار زیرلایه تحت تأثیر مثبت کاربرد هر دو تکنیک مهندسی سطح، شامل پاشش پوشش سرامیکی و اصلاح سطح با عملیات ذوب مجدد لیزری، قرار گرفته است. این بهبود به دلیل تشکیل سطوح زیست فعال و مقاوم‌تر است. اصلاح سطح دو عملکرد انجام می‌دهد. عملکرد اول به عنوان مانعی عمل می‌کند که از رسیدن مایعات بدن به ایمپلنت جلوگیری می‌کند و همچنین زبری و تخلخل سطحی مشابه زبری سطح استخوان را برای رشد بافت اطراف فراهم می‌کند.